Dissociative and Reactive Hyperthermal Ion−Surface Collisions with Langmuir−Blodgett Films Terminated by $CF_3(CH_2)_n$−, *n*-Perfluoroalkyl, or *n*-Alkyl Groups

Chungang Gu,[†] Vicki H. Wysocki,*[,†] Atsuhiro Harada,[‡] Hiroaki Takaya,[‡] and Itsumaro Kumadaki[‡]

Contribution from the Department of Chemistry, University of Arizona, Tucson, Arizona 85721, and Faculty of Pharmaceutical Sciences, Setsunan University, Osaka 573-01, Japan

Received March 5, 1999

Abstract: Langmuir−Blodgett (L−B) films prepared from 18,18,18-trifluorooctadecanoic acid [$CF_3(CH_2)_{16}$-COOH], perfluorotetradecanoic acid [*n*-$C_{13}F_{27}$COOH], or octadecanoic acid [*n*-$C_{17}H_{35}$COOH] were used as target surfaces for hyperthermal ion−surface collisions. The synthesis of 18,18,18-trifluorooctadecanoic acid and the preparation of the L−B film from this compound using a subphase containing Al^{3+} are reported in this paper. The Ion−surface collision results show that the outermost surface group, namely CF_3 vs CH_3, is the main determinant for the efficiency of both energy transfer and electron transfer during low-energy (e.g., 10−100 eV) polyatomic ion−surface collisions. For atomic projectile ions, there is evidence of penetration into a depth of the films.

Introduction

Gas-phase ion−surface interactions are of interest because of both their practical applications and the fascinating fundamental chemistry and physics associated with the collision processes. Investigations of these interactions may be viewed as falling into two categories if based on the range of collision energies applied: low energy (e.g., a few eV to a couple of hundred eV) and high energy (e.g., 1 keV to several hundred keV). For example, keV projectile ions (often atomic ions) can impart their energy and momentum to the surface species causing sputtering, or penetrate into the solid surface and become implanted there. Ion sputtering from the surface is exploited for the analysis of chemical composition of surfaces in the established technique of secondary ion mass spectrometry (SIMS).[1] Ion implantation is investigated for fabrication of semiconductor materials and optical films.[2] The studies presented here belong to the low-energy category of ion−surface interactions. The physical chemistry and physics associated with fundamental processes involving low-energy collisions of small ions (e.g., up to a few atoms) with crystal surfaces have been active research areas.[3] More recently, collisions of polyatomic ions with organic thin film surfaces have been investigated. Dramatic differences are seen between low-energy ion−surface collisions and those in the keV range. For example, some polyatomic projectiles may survive the collision at lower energies (e.g., 5 eV) and "soft-land" as "molecular parachutes" on a fluorinated organic surface.[4] There are also several other aspects of interest to chemists in this range of collision energies. One is dissociative scattering of polyatomic projectile ions. This led to the development of surface-induced dissociation (SID) by Cooks and co-workers.[5−7] SID is not only an alternative to CID (collision-induced dissociation)[8] in tandem mass spectrometry (MS/MS)[9,10] with the gaseous target (in CID) replaced by a surface target (in SID) for ion activation, but SID also brings some special features to MS/MS studies. In particular, SID provides higher transfer of kinetic energy into internal modes of polyatomic projectile ions (i.e., T → V), and provides narrower distributions of the internal energies deposited into the ions (compared to CID).[6] These two features result in easily tunable internal energies of polyatomic projectile ions activated by SID. The ion chemistry implications of these characteristics of SID include the following: (i) effective fragmentation for some refractory ions (either large[11,12] or very stable[13] ions), (ii) mechanistic insights drawn from energetic studies,[14,15] and (iii) extraction of activation energies for some ion fragmentation pathways.[16,17]

Another interesting chemical aspect of low-energy ion−surface interactions is reaction between the gas-phase projectile ions and the target surfaces. For example, abstractions of C_nH_m and/or H from hydrocarbon-terminated surfaces[6,13,18−26] and F (single or multiple) from fluorinated surfaces[18,21,27,28] can occur

* To whom correspondence should be addressed. Tel: (520)621-2628. Fax: (520)621-8407. E-mail: vwysocki@u.arizona.edu.
[†] University of Arizona.
[‡] Setsunan University.

(1) (a) Czanderna, A. W.; Hercules, D. M. *Ion Spectroscopies For Surface Analysis*; Plenum Press: New York, 1991. (b) Winograd, N. *Anal. Chem.* **1993**, *65*, 622A−629A. (c) Benninghoven, A.; Hagenhoff, B.; Niehuis, E. *Anal. Chem.* **1993**, *65*, 630A−640A.

(2) (a) Rimini, E. *Ion implantation: basics to device fabrication*; Kluwer Academic Publishers: Boston, 1995. (b) Townsend, P. D.; Chandler, P. J.; Zhang, L. *Optical effects of ion implantation*; Cambridge University Press: Cambridge, UK, 1994. (c) Shi, J.; Kikkawa, J. M.; Proksch, R.; Schaffer, T.; Awschalom, D. D.; Medeirosribeiro, G.; Petroff, P. M. *Nature* **1995**, *377*, 707−710. (d) Narayan, J.; Godbole, V. P.; White, C. W. *Science* **1991**, *252*, 416−418.

(3) Rabalais, J. W. *Low energy ion-surface interactions*; John Wiley: New York, 1994.

(4) Miller, S. A.; Luo, H.; Pachuta, S. J.; Cooks, R. G. *Science* **1997**, *275*, 1447−1450.

(5) Mabud, M. D. A.; Dekrey, M. J.; Cooks, R. G. *Int. J. Mass Spectrom. Ion Process.* **1985**, *67*, 285−294.

(6) Cooks, R. G.; Ast, T.; Mabud, A. *Int. J. Mass Spectrom. Ion Process.* **1990**, *100*, 209−265.

(7) Cooks, R. G.; Miller, S. A.; Ast, T.; Feng, B.; Pradeep, T. *Adv. Mass Spectrom.* **1995**, *13*, 179−197.

(8) McLuckey, S. A. *J. Am. Soc. Mass Spectrom.* **1992**, *3*, 599−614.

10.1021/ja990719a CCC: $18.00
Published on Web 10/30/1999

with some projectile ions. Certain projectiles react with organized organic thin films to provide spectral features that reflect the film quality.[22] The potential to probe the outermost surface groups or atoms by certain polyatomic ion−surface reactions has been shown.[25] In addition to the reaction products scattered off surfaces, reaction products are sometimes formed on the target surface, and the potential of ion−surface reactions in the modification of organic surfaces is being investigated[29,30]

One of the important developments in surface-induced dissociation is the use of organic thin films on metals as the collision targets (e.g., self-assembled monolayers (SAMs) of *n*-alkanethiols on gold or silver).[31,32] Organic thin films such as SAMs provide control of the chemical properties of the target surface. The thin film provides a barrier to electron transfer and thus limits the neutralization of projectile ions that otherwise would occur readily on a bare metal,[18,21] without the charge accumulation that would occur on an insulator surface.[33] Fluorinated thin films show some practical advantages as the collision targets. It is known that increased T → V and decreased neutralization of projectile ions occur on fluorinated surfaces relative to hydrocarbon-terminated surfaces. These differences have been reported for ordered thin films such as SAMs of fluoroalkanethiols [e.g., $CF_3(CF_2)_nCH_2CH_2SH$, $n = 7, 11$] vs *n*-alkanethiols on gold,[18,21] and thin films of a liquid perfluoropolyether (PFPE) vs pump oil residue on metal.[34,35] An impulsive excitation is suggested in the literature as a dominant mechanism for internal energy deposition into a *polyatomic* projectile ion during its collision, in particular, with organic thin films on metal.[7,36,37] Charge transfer-induced electronic excitation has also been reported (e.g., CF_3^+ collisions with a metal surface,[38] in addition to many diatomic ion collisions with crystal surfaces[3]). It has been suggested by several authors[13,18,31,34,36,39] that the difference in energy transfer occurring with fluorinated vs hydrocarbon-terminated surfaces is due to the different effective masses of target surface species. The molecular beam scattering experiments with liquid films by Nathanson and co-workers show that the energy transfer to the film is dependent on the mass of both partners of the collision (i.e., mass of the gaseous impinging molecule and effective mass of the surface).[39] A large influence of the azimuthal orientation of a single-crystal surface indicated the importance of direct momentum transfer.[38] The dependence of internal energy deposition ratio on the size and shape of projectile ions was suggested as due to the effective mass of the surface contacted at the moment of impact.[23]

The experiments in this study are designed to investigate (i) whether the *difference* in internal energy deposition into projectile ions with fluorinated and hydrocarbon terminated surfaces is mainly caused by the rigidity of $(CF_2)_n$ vs $(CH_2)_n$ or the mass (momentum) effect of *terminal* fluorine vs hydrogen and (ii) whether the *difference* in neutralization of projectile ions is mainly controlled by the exposed surface groups (e.g., *terminal* CF_3 vs CH_3). Answers to these two questions will add to our fundamental understanding of ion−surface interactions. The CF_3-terminated model surface also raises an additional interesting point. It provides a convenient model surface for further experimental examination of the proposed mechanism of multiple fluorine additions to an atomic transition metal projectile ion.[28]

The present study compares the results obtained with a model surface terminated by a $CF_3(CH_2)_n$- group to those obtained with *n*-perfluoroalkyl- or *n*-alkyl-terminated surfaces. Langmuir−Blodgett (L−B) films[40,41] were utilized in this study. In the 1930s, Irving Langmuir and Katharine B. Blodgett discovered the technique of transferring monomolecular films of amphiphilic molecules (e.g., fatty acids or their dicovalent metal salts) from an air−water interface to a solid substrate (e.g., a glass or metal plate) to form a monolayer or a builtup multilayer by dipping procedures. Since then, comprehensive investigations made on L−B films for diverse purposes using a great variety of amphiphilic molecules have been described in many books and review papers, including several excellent recent ones.[40,41] In a Communication to this journal in 1997, we reported, by using isotopically labeled L−B films, that low-energy ion−surface reactions of organic projectiles predominantly involve

(9) Busch, K. L.; Glish, G. L.; McLuckey, S. A. *Mass Spectrometry/Mass Spectromety: Techniques and Application of Tandem Mass Spectrometry*; VCH Publishers: New York, 1988.
(10) de Hoffmann, E. *J. Mass Spectrom.* **1996**, *31*, 129−137.
(11) Chorush, R. A.; Little, D. P.; Beu, S. C.; Wood, T. D.; McLafferty, F. W. *Anal. Chem.* **1995**, *67*, 1042−1046.
(12) Dongré, A. R.; Somogyi, Á.; Wysocki, V. H. *J. Mass Spectrom.* **1996**, *31*, 339−350.
(13) Callahan, J. H.; Somogyi, Á.; Wysocki, V. H. *Rapid Commun. Mass Spectrom.* **1993**, *7*, 693−699.
(14) Beck, R. D.; St. John, P.; Homer, M. L.; Whetten, R. L. *Science* **1991**, *253*, 879−883.
(15) Dongré, A. R.; Jones, J. L.; Somogyi, Á.; Wysocki, V. H. *J. Am. Chem. Soc.* **1996**, *118*, 8365−8374.
(16) Wainhaus, S. B.; Gislason, E. A.; Hanley, L. *J. Am. Chem. Soc.* **1997**, *119*, 4001−4007.
(17) Weis, P.; Rockenberger, J.; Beck, R. D.; Kappes, M. M. *J. Chem. Phys.* **1996**, *104*, 3629−3637.
(18) Morris, M. R.; Riederer, D. E.; Winger, B. E.; Cooks, R. G.; Ast, T.; Chidsey, C. E. D. *Int. J. Mass Spectrom. Ion Process.* **1992**, *122*, 181−217.
(19) Williams, E. R.; Jones, G. C.; Fang, L.; Zare, R. N.; Garrison, B. J.; Brenner, D. W. *J. Am. Chem. Soc.* **1992**, *114*, 3207−3210.
(20) Wu, Q. Y.; Hanley, L. *J. Am. Chem. Soc.* **1993**, *115*, 1191−1193.
(21) Somogyi, Á.; Kane, T. E.; Ding, J. M.; Wysocki, V. H. *J. Am. Chem. Soc.* **1993**, *115*, 5275−5283.
(22) Kane, T. E.; Somogyi, Á.; Wysocki, V. H. *Org. Mass Spectrom.* **1993**, *28*, 1665−1673.
(23) Beck, R. D.; Rockenberger, J.; Weis, P.; Kappes, M. M. *J. Chem. Phys.* **1996**, *104*, 3638−3650.
(24) Hayward, M. J.; Park, F. D. S.; Phelan, L. M.; Bernasek, S. L.; Somogyi, Á.; Wysocki, V. H. *J. Am. Chem. Soc.* **1996**, *118*, 8375−8380.
(25) Gu, C.; Wysocki, V. H. *J. Am. Chem. Soc.* **1997**, *119*, 12010−12011.
(26) Phelan, L. M.; Hayward, M. J.; Flynn, J. C.; Bernasek, S. L. *J. Phys. Chem. B* **1998**, *102*, 5667−5672.
(27) Pradeep, T.; Ast, T.; Cooks, R. G.; Feng, B. *J. Phys. Chem.* **1994**, *98*, 9301−9311.
(28) Pradeep, T.; Riederer, D. E.; Hoke, S. H.; Ast, T.; Cooks, R. G.; Linford, M. R. *J. Am. Chem. Soc.* **1994**, *116*, 8658−8665.
(29) Pradeep, T.; Feng, B.; Ast, T.; Patrick, J. S.; Cooks, R. G.; Pachuta, S. J. *J. Am. Soc. Mass Spectrom.* **1995**, *6*, 187−194.
(30) Ada, E. T.; Kornienko, O.; Hanley, L. *J. Phys. Chem. B* **1998**, *102*, 3959−3966.
(31) Winger, B. E.; Julian, R. K.; Cooks, R. G.; Chidsey, C. E. D. *J. Am. Chem. Soc.* **1991**, *113*, 8967−8969.
(32) Wysocki, V. H.; Jones, J. L.; Ding, J. M. *J. Am. Chem. Soc.* **1991**, *113*, 8969−8970.
(33) Kane, T. E.; Wysocki, V. H. *Int. J. Mass Spectom. Ion Process.* **1994**, *140*, 177−184.
(34) Pradeep, T.; Miller, S. A.; Cooks, R. G. *J. Am. Soc. Mass Spectrom.* **1993**, *4*, 769−773.
(35) Schey, K. L.; Durkin, D. A.; Thornburg, K. R. *J. Am. Soc. Mass Spectrom.* **1995**, *6*, 257−263.
(36) Burroughs, J. A.; Wainhaus, S. B.; Hanley, L. *J. Phys. Chem.* **1994**, *98*, 10913−10919.
(37) Ast, T.; Riederer, D. E.; Miller, S. A.; Morris, M.; Cooks, R. G. *Org. Mass Spectrom.* **1993**, *28*, 1021−1033.
(38) Koppers, W. R.; Beijersbergen, J. H. M.; Tsumori, K.; Weeding, T. L.; Kistemaker, P. G.; Kleyn, A. W. *Phys. Rev. B* **1996**, *53*, 207−209.
(39) Saecker, M. E.; Govoni, S. T.; Kowalski, D. V.; King, M. E.; Nathanson, G. M. *Science* **1991**, *252*, 1421−1424.
(40) (a) Ulman, A. *Characterization of Organic Thin Films*; Butterworth-Heinemann: Boston, 1995. (b) Ulman, A. *An introduction to ultrathin organic films: from Langmuir−Blodgett to self-assembly*; Academic Press: Boston, 1991. (c) Petty, M. C. *Langmuir−Blodgett films: an introduction*; Cambridge University Press: Cambridge, UK, 1996.
(41) (a) Zasadzinski, J. A.; Viswanathan, R.; Madsen, L.; Garnaes, J.; Schwartz, D. K. *Science* **1994**, *263*, 1726−1733. (b) Peterson, I. R. *J. Phys. D: Appl. Phys.* **1990**, *23*, 379−395.

the outermost surface groups (e.g., terminal methyl group on $^{13}CH_3(CH_2)_{16}COOH$ or $CD_3(CH_2)_{16}COOH$ L−B film).[25] A reason for our choice of the L−B films for the present study, quite similar to that in our previous Communication, is that the material to make the desired surface (i.e., $CF_3(CH_2)_n$-terminated L−B film) is available, whereas the materials for making equivalent SAM surfaces were not available when we began this study.[42] Recently, characterizations of SAM surfaces prepared from $CF_3(CH_2)_nSH$ (n = 9−15) have been reported.[43,44] Terminally fluorinated fatty acids, 18,18,18-trifluorooctadecanoic acid and 12,12,12-trifluorododecanoic acid, were synthesized initially for ^{19}F NMR studies of the stabilizing effect of vitamin E on liposome membranes.[45] The synthesis of 18,18,18-trifluorooctadecanoic acid, $CF_3(CH_2)_{16}COOH$, and its use in the investigation of ion−surface interactions are reported here.

Experimental Sections

(A) Synthesis of 18,18,18-Trifluorooctadecanoic Acid and 12,-12,12-Trifluorododecanoic Acid. The experiments at Setsunan University, Japan, for synthesis and purification of these two acids are as follows.

Methyl 12,12,12-Trifluoro-10-iodododecanoate (2). Methyl 10-undecenoate (**1**, 8.72 g, 44.0 mmol) was dissolved in MeOH (20.0 mL). This solution and Raney Ni (W-2) (2.09 g) were then sealed in a stainless steel tube. The tube was cooled to −78 °C, and CF_3I (6.50 mL) was added using a vacuum line. The tube was sealed and stirred at 80 °C for 20 h. After the catalyst was filtered off, the solvent was evaporated under vacuum, and the residue was dissolved in CH_2Cl_2. The CH_2Cl_2 layer was washed with saturated $NaHCO_3$ and dried over $MgSO_4$. After evaporation of the solvent, the residue was distilled to give methyl 12,12,12-trifluoro-10-iodododecanoate (**2**, 16.43 g, 95%). **2**: Colorless oil. Bp 103.0 °C/0.0190 mmHg. MS *m*/*z* 394 (M^+). HRMS Calcd for $C_{13}H_{22}F_3IO_2$ (M^+) 394.062; found 394.063. IR (neat) cm^{-1} 2932, 2864 (C−H), 1742 (*CO*OCH$_3$). ^1H NMR ($CDCl_3$) δ 1.15−1.45 (10H, b), 1.62 (2H, quin, J = 7.3 Hz), 1.75 (2H, m), 2.30 (2H, t, J = 7.6 Hz), 2.83 (2H, m), 3.67 (3H, s), 4.19 (1H, m). ^{19}F NMR ($CDCl_3$) ppm (from $C_6H_5CF_3$) −1.12 (3F, t, J = 10.3 Hz).

Methyl 12,12,12-Trifluorododecanoate (3). Zn (1.97 g, 30.1 mmol) $NiCl_2 \cdot 6H_2O$ (0.36 g, 1.50 mmol), and H_2O (5 dr) were stirred in THF (25 mL) for 15 min in a stream of Ar, and methyl 12,12,12-trifluoro-10-iodododecanoate (**2**, 5.85 g, 14.8 mmol) was added to this mixture. After the mixture was stirred at room temperature for 3 h, it was poured into saturated $NaHCO_3$. After the mixture was stirred for 30min, it was filtered through a Celite layer. The layer was washed with Et_2O. The filtrate and washings were combined and extracted with Et_2O. The Et_2O layer was washed with H_2O, dried over $MgSO_4$, and concentrated under vacuum. The residue was separated by column chromatography (SiO_2, hexane−Et_2O, 9:1) to give methyl 12,12,12-trifluorododecanoate (**3**, 3.75 g, 94%). **3**: Colorless oil. MS *m*/*z* 268 (M^+). HRMS Calcd for $C_{13}H_{23}F_3O_2$ (M^+) 268.165; found 268.166. IR (neat) cm^{-1} 2936, 2864 (C−H), 1744 (*CO*OCH$_3$). ^1H NMR ($CDCl_3$) δ 1.15−1.45 (14H, b), 1.58 (2H, m), 2.05 (2H, qt, J = 10.6, 7.5 Hz), 2.30 (2H, t, J = 7.6 Hz), 3.66 (3H, s). ^{19}F NMR ($CDCl_3$) ppm −3.42 (3F, t, J = 10.6 Hz).

12,12,12-Trifluoro-1-dodecanol (4). A solution of methyl 12,12,-12-trifluorododecanoate (**3**, 2.70 g, 10.1 mmol) in Et_2O (10.0 mL) was dropped into a suspension of $LiAlH_4$ (0.458 g, 12.1 mmol) in Et_2O (20.0 mL) at room temperature in an atmosphere of Ar, and the mixture was stirred at room temperature for 5 h. The mixture was treated with ice, then 10% H_2SO_4 was added slowly until $Al(OH)_3$ dissolved, and extracted with Et_2O. The Et_2O layer was washed with saturated NaCl, dried over $MgSO_4$, and concentrated under vacuum. The residue was purified by column chromatography (SiO_2, CH_2Cl_2−MeOH, 99:1) to give 12,12,12-trifluoro-1-dodecanol (**4**, 2.40 g, 99%). **4**: Colorless crystals. Mp 42.0 °C. MS *m*/*z* 222 (M^+ − OH). HRMS Calcd for $C_{12}H_{21}F_3$ (M^+ − OH) 222.160; found 222.160. IR (KBr) cm^{-1} 3700−3200 (O−H), 2928, 2860 (C−H). ^1H NMR ($CDCl_3$) δ 1.15−1.45 (15H, b), 1.56 (4H, m), 2.05 (2H, qt, J = 10.6, 7.5 Hz), 3.64 (2H, t, J = 6.6 Hz). ^{19}F NMR ($CDCl_3$) ppm −3.42 (3F, t, J = 10.6 Hz).

1-Bromo-12,12,12-trifluorododecane (5). Concentrated H_2SO_4 (7.60 mL) and 48% HBr (30.0 mL) were added to 12,12,12-trifluoro-1-dodecanol (**4**, 9.77 g, 40.67 mmol) alternatingly under ice-cooling, and the mixture was refluxed at 135 °C for 5 h. After cooling, the mixture was extracted with CH_2Cl_2. The CH_2Cl_2 layer was washed with H_2O then with saturated $NaHCO_3$, dried over $MgSO_4$, and concentrated under vacuum. The residue was purified by column chromatography (SiO_2, hexane) to give 1-bromo-12,12,12-trifluorododecane (**5**, 12.27 g, 99%). **5**: Pail yellow oil. Bp 114.0 °C/5.00 mmHg. MS *m*/*z* 302 (M^+), 304 (M + 2). HRMS Calcd for $C_{12}H_{22}BrF_3$ (M^+) 302.086; found 302.087. IR (neat) cm^{-1} 2932, 2860 (C−H). ^1H NMR ($CDCl_3$) δ 1.15−1.49 (14H, b), 1.55 (2H, t, J = 7.0, 6.7 Hz), 1.85 (2H, tt, J = 7.3, 7.2 Hz), 2.05 (2H, qt, J = 10.6, 7.5 Hz), 3.40 (2H, t, J = 7.0 Hz). ^{19}F NMR ($CDCl_3$) ppm −3.42 (3F, t, J = 10.6 Hz).

1-(12,12,12-Trifluorododecyl)cyclohexanol (6). In an atmosphere of Ar, 1-bromo-12,12,12-trifluorododecane (**5**, 0.010 g, 0.033 mmol) was added to a suspension of Li (0.054 g, 7.78 mmol) in Et_2O (4.0 mL), and the mixture was immersed in an ultrasonic bath till the reaction started (about 10 min). After the reaction started, a solution of 1-bromo-12,12,12-trifluorododecane (**5,** 1.00 g, 3.32 mmol) in Et_2O (10.0 mL) was added dropwise in 3.5 h, then the mixture was stirred for an additional 1 h. After cyclohexanone (0.70 mL, 6.75 mmol) was added to this mixture, it was stirred at room temperature overnight. The mixture was poured into ice−water, neutralized with 10% HCl, then extracted with Et_2O. The Et_2O layer was washed with saturated NaCl, dried over $MgSO_4$, and concentrated under vacuum. The residue was purified by column chromatography (SiO_2, hexane−CH_2Cl_2, 7:3) to give 1-(12,12,12-trifluorododecyl)cyclohexanol (**6**, 0.431 g, 40%). **6**: Yellow oil. MS *m*/*z* 322 (M^+). HRMS Calcd for $C_{18}H_{33}F_3O$ (M^+) 322.248; found 322.249. IR (neat) cm^{-1} 3600−3200 (O−H), 2932, 2860 (C−H). ^1H NMR ($CDCl_3$) δ 1.15−1.75 (31H, b), 2.05 (2H, qt, J = 10.3, 7.5 Hz). ^{19}F NMR ($CDCl_3$) ppm −3.42 (3F, t, J = 10.3 Hz).

18,18,18-Trifluoro-6-oxooctadecanoic Acid (7). To a solution of 1-(12,12,12-trifluorododecyl)cyclohexanol (**6**, 1.52 g, 4.73 mmol) in acetic acid (55.0 mL) was added CrO_3 (0.379 g, 3.79 mmol) with vigorous stirring for 10 min. Then CrO_3 (4.13 g, 41.3 mmol) was added slowly keeping the mixture under 30 °C by ice-cooling. After the mixture was stirred for 3 h, H_2O (50.0 mL) was added, and the mixture was extracted with Et_2O. The Et_2O layer was washed by water, then extracted with 5% NaOH. The aqueous layer was acidified with 36% HCl and extracted with Et_2O. The Et_2O layer was dried over $MgSO_4$ and concentrated under vacuum. The residue was recrystallized from hexane to give 18,18,18-trifluoro-6-oxooctadecanoic acid (**7**, 0.773 g, 46.4%). **7**: Colorless plates. Mp 52.0−53.0 °C. MS *m*/*z* 352 (M^+). IR (KBr) cm^{-1} 3650−3200 (O−H), 2920, 2856 (C−H), 1734, 1710 (*CO*OH, *C*=*O*), ^1H NMR ($CDCl_3$) δ 1.15−1.88 (14H, b), 2.07 (2H, m), 2.37 (4H, m), 2.47 (2H, t, J = 7.3 Hz).^{19}F NMR ($CDCl_3$) ppm −3.42 (3F, t, J = 10.1 Hz).

18,18,18-Trifluorooctadecanoic Acid (8). A suspension of Zn (1.40 g, 21.3 mmol) and $HgCl_2$ (0.124 g, 0.457 mmol) in 36% HCl (0.60 mL) and H_2O (15.0 mL) was stirred for 5 min. After the surface of Zn was amalgamated, the aqueous phase was decanted off. To this Zn, H_2O (4.00 mL), 36% HCl (11.0 mL), toluene (6.40 mL), and 18,18,-18-trifluoro-6-oxooctadecanoic acid (**7**, 0.154 g, 0.437 mmol) were added in this order, and the mixture was refluxed for 30 h under vigorous stirring. To keep the acidity of the medium, 36% HCl (0.50 mL) was added every 6 h. The mixture was diluted with H_2O and extracted with Et_2O. The Et_2O layer was washed with H_2O, dried over $MgSO_4$, and concentrated under vacuum. The residue was recrystallized from hexane to give 18,18,18-trifluorooctadecanoic acid (**8**, 0.042 g, 28%). **8**: Colorless plates. Mp 68.7−69.0 °C. MS *m*/*z* 338 (M^+). HRMS

(42) Gu, C.; Angelico, V. J.; Wysocki, V. H.; Harada, A.; Takaya, H.; Kumadaki, I. *Proceedings of The 46th ASMS Conference on Mass Spectrometry and Applied Topics*; Orlando, FL, 1998.

(43) Miura, Y. F.; Takenaga, M.; Koini, T.; Graupe, M.; Garg, N.; Graham, R. L.; Lee, T. R. *Langmuir* **1998**, *14*, 5821−5825.

(44) Houssiau, L.; Graupe, M.; Colorado, R.; Kim, H. I.; Lee, T. R.; Perry, S. S.; Rabalais, J. W. *J. Chem. Phys.* **1998**, *109*, 9134−9147.

(45) Nishimura, M.; Koyama, M.; Takagi, T.; Ando, A.; Kumadaki, I.; Urano, S. *Bitamin E kenkyu no shimpo (Progress in Studies on Vitamin E* (Japanese); Sankyo Shuppan: Tokyo, 1995; Vol. V.

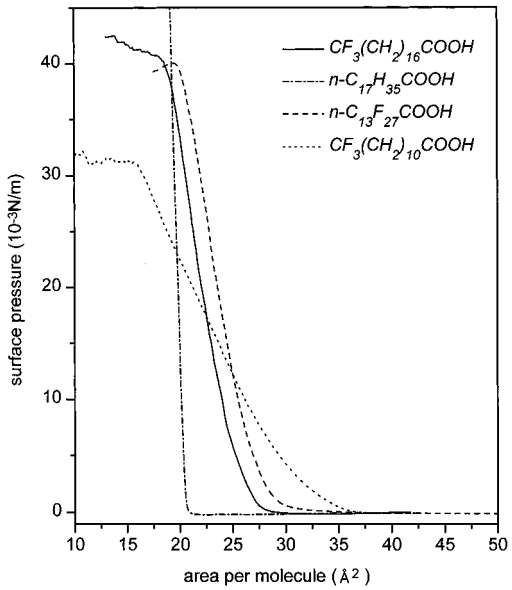

Figure 1. Surface pressure as a function of surface area (i.e., Langmuir isotherms), measured at room temperature in a L−B trough, with 5×10^{-5} M Al^{3+} in water as the subphase for $CF_3(CH_2)_{16}COOH$, $CF_3(CH_2)_{10}$-COOH, and n-$C_{13}F_{27}COOH$ and with 5×10^{-4} M Cd^{2+} in water as the subphase for stearic acid.

Calcd for $C_{18}H_{33}F_3O_2$ (M^+) 338.243; found 338.242. IR (KBr) cm^{-1} 3700−3300 (O−H), 2920, 2852 (C−H), 1706 (*CO*OH). ^{1}H NMR ($CDCl_3$) δ 1.15−1.45 (24H, b), 1.55 (2H, quin, $J = 7.8$ Hz), 1.64 (2H, quin, $J = 7.2$ Hz), 2.07 (2H, qt, $J = 10.1$, 7.5 Hz). ^{19}F NMR ($CDCl_3$) ppm −3.42 (3F, t, $J = 10.1$ Hz).

12,12,12-Trifluorododecanoic acid (**9**) was converted from methyl 12,12,12-trifluorooctadecanoate (**3**) via NaOH catalyzed hydrolysis followed by acidification. **9**: Colorless wool. Mp 49.5−50.0 °C. MS *m*/*z* 254 (M^+). HRMS Calcd. for $C_{12}H_{21}F_3O_2$ (M^+) 254.149; found 254.149. IR (KBr) cm^{-1} 3700−2200 (O−H), 2928, 2860 (C−H), 1702 (*CO*OH). ^{1}H NMR ($CDCl_3$) δ 1.15−1.45 (14H, b), 1.58 (2H, m), 2.05 (2H, qt, $J = 11.0$, 7.50 Hz), 2.30 (2H, t, $J = 7.63$ Hz). ^{19}F NMR ($CDCl_3$) ppm −3.42 (3F, t, $J = 11.0$ Hz).

(B) Preparation of L−B Films. The preparation of the L−B film from octadecanoic acid (n-$C_{17}H_{35}COOH$, stearic acid) follows a well-established "textbook" method with Cd^{2+} as the counterion in the aqueous subphase (5×10^{-4} M $CdCl_2$).[40] The preparation of the L−B film from perfluorotetradecanoic acid (n-$C_{13}F_{27}COOH$) follows the method of Nakahama et al.,[46] who first successfully deposited the L−B film of a perfluorinated fatty acid (e.g., n-$C_{10}F_{21}COOH$) by using a subphase containing Al^{3+}. We have found that a well-packed monolayer of 18,18,18-trifluorooctadecanoic acid forms on 5×10^{-5} M Al^{3+} ($AlCl_3$) aqueous subphase, the same subphase used by Nakahama et al. for a perfluorinated fatty acid.[46] It is noteworthy that we found no packed monolayer of 18,18,18-trifluorooctadecanoic acid forms on the subphase of either Cd^{2+} (0.5 mM $CdCl_2$) or 0.01 M HCl aqueous solution which are two typical subphases[40] used for making L−B films with "normal" fatty acids. Figure 1 gives the surface pressure as a function of area per molecule (i.e., $\pi \sim A$, Langmuir isothermal curve), measured in a L−B trough with 18,18,18-trifluorooctadecanoic acid molecules on the air−water interface. The measured isothermal curves for stearic acid and perfluorotetradecanoic acid are provided as dashed lines in Figure 1 for comparison. The isothermal curve of 12,12,12-trifluorododecanoic acid, which has a shorter chain length than 18,-18,18-trifluorooctadecanoic acid, is also provided in Figure 1. Note this shorter chain length ω,ω,ω-trifluoroalkanoic acid does not form a close-packed ("solid phase") monolayer on the air−water interface.[47]

Three-layer Y-type L−B films, with the hydrophobic end as the terminal group at the vacuum−film interface, were used in our ion−surface collision experiments. A Y-type multilayer L−B film is that with hydrophobic−hydrophobic or hydrophilic−hydrophilic interactions between two adjacent layers (i.e., tail-to-tail, head-to-head), built when a vertically oriented substrate surface is repeatedly pulled-up and pushed-down through the monomolecular film on the air−water interface.[40] The L−B films were deposited in a NIMA (Type-611, England) L−B trough. The amphiphilic carboxylic acid molecules were spread onto the water−air interface in a 0.1−1 mM solution of chloroform (HPLC grade). The surface pressure of the monolayer during the deposition was maintained at 32×10^{-3}, 27×10^{-3}, and 23×10^{-3} N·m^{-1} for n-$C_{17}H_{35}COOH$, n-$C_{13}F_{27}COOH$, and $CF_3(CH_2)_{16}COOH$ L−B films (*hereafter referred to as* ***stearate***, ***perfluorinated,*** *and* ***CF_3-$(CH_2)_n$-terminated*** *L−B films, respectively*). The dipping speed of the metal substrate was kept at 3 mm·min^{-1}. Stearic acid (99%) and perfluoroteradecanoic acid (97+%) were purchased from Aldrich and used without further purification. The high-purity water ([conductivity]$^{-1} \geq 18$ MΩ·cm) used for the subphase in the L−B trough was generated by a Nanopure (Barnstead, Dubuque, IA) or a Milli-Q-plus (Millipore, Bedford, MA) ultrapure water system. Mechanically polished aluminum plates, cleaned by ultrasonicating in various organic solvents after the plates were exposed to air for a few hours (the presence of oxide is presumed and desirable), were used as the substrates of the L−B films. The L−B films prepared (the film covering area on the substrate was as large as 20 mm × 30 mm) were put in a surface holder and stayed in the vacuum chamber (of the instrument described below) overnight before ion−surface collision experiments.

(C) Ion−Surface Collision Experiments. Ion−surface collisions were carried out on a SID tandem mass spectrometer that has been described previously.[12,48] Briefly, the mass spectrometer consists of two Extrel (now ABB Extrel, Pittsburgh, PA) 4000 amu quadrupole mass analyzers positioned at 90° relative to each other, with the surface bisecting the two quadrupoles. The precursor ions used in this study were all generated in an electron impact ionization (EI) source. All chemicals used to generate projectile ions, except C_{60}, were introduced into the EI source region through a needle valve inlet attached to a sample reservoir. C_{60} was introduced by thermal desorption at 400 °C from a direct probe for solids. The atomic metal ions (e.g., Mo^+, Cr^+) used in the experiments were generated from the metal hexacarbonyls by EI. The beam of precursor ion that are mass selected by the first quadrupole was incident onto the surface at roughly 45° to the surface normal. Product ions resulting from collisions with surfaces were collected by focusing electrostatic-lenses and analyzed by the second quadrupole. The collision energy was determined by the potential difference, between the EI source block and the target surface, multiplied by the charge of the ion. The SID instrument has a surface holder that can carry several surfaces, which makes it possible to obtain results for different surfaces under the same instrumental conditions by moving each surface into the ion path. The ion beam density is less than 1 nA in a 0.5 cm^2 area [49] of the ion−surface impact. In the experiments of the present study, each film was used for 10−30 min in ion−surface collisions. Note that the "static" limit of $\sim 10^{12}$ ions/cm^2 in SIMS[1] may not be applied here, because the collision energies in our study are much lower than those in SIMS.

Results and Discussion

Different chemistry occurs when organic projectile ions collide with flurocarbon vs hydrocarbon terminated organic thin films (L−B films in the present study). Several sets of experimental data are presented and discussed below that are aimed at determining the effect of different terminal surface groups (namely CF_3 vs CH_3) on the different chemistry of hyperthermal ion−surface interactions. The experimental data include those for internal energy deposition, electron transfer, and ion−surface reaction. Also provided are comparisons of

(46) Nakahama, H.; Miyata, S.; Wang, T. T.; Tasaka, S. *Thin Solid Films* **1986**, *141*, 165−169.

(47) This is not surprising. The longer the amphiphilic molecule, the better the quality of the L−B film. For example, to prepare a vinyl-terminated L−B film, naturally occurring CH_2═$CH(CH_2)_8COOH$ had to be expanded to CH_2═$CH(CH_2)_{20}COOH$ by chemical synthesis, see: Barraud, A.; Rosilio, C.; Ruaudel-Teixier, A. *J. Colloid Interface Sci.* **1977**, *62*, 509−523.

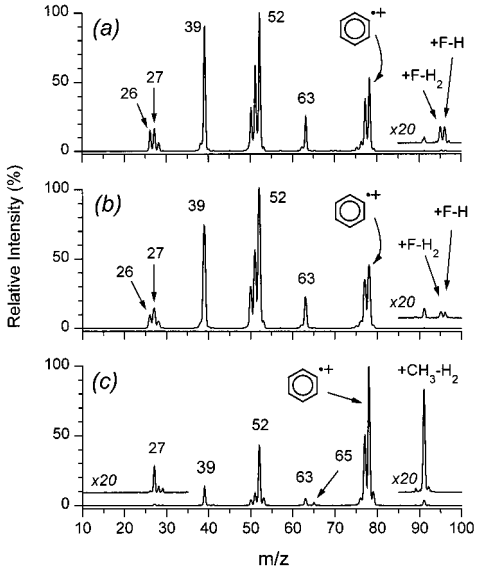

Figure 2. The product ion spectra acquired when benzene molecular ion (*m*/*z* 78) collides at 30 eV kinetic energy with Y-type three-layer L−B films prepared from (a) *n*-$C_{13}F_{27}COOH$ (Al^{3+} salt), (b) $CF_3(CH_2)_{16}$-COOH (Al^{3+} salt), and (c) *n*-$C_{17}H_{35}COOH$ (Cd^{2+} salt).

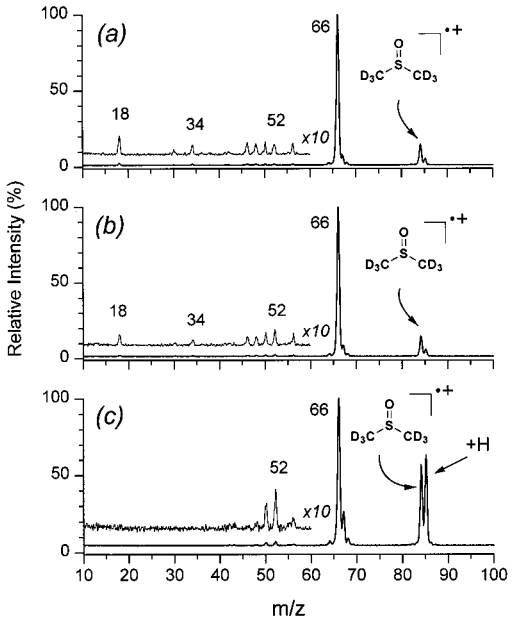

Figure 3. The product ion spectra acquired when dimethyl sulfoxide-d_6 (DMSO-d_6) molecular ion (*m*/*z* 84) collides at 20 eV kinetic energy with (a) *n*-$C_{13}F_{27}COOH$, (b) $CF_3(CH_2)_{16}COOH$, and (c) *n*-$C_{17}H_{35}$ COOH L−B films.

data for polyatomic ions vs atomic ions, and lower collision energies (e.g., <100 eV) vs a slightly higher energy (e.g., 220 eV).

Transfer of Kinetic Energy into Internal Modes for Polyatomic Projectile Ions. The energy deposition at collision energies <100 eV was investigated by using several different projectile ion probes: e.g., benzene molecular ion, dimethyl sulfoxide-d_6 (DMSO-d_6) molecular ion, and tungsten hexacarbonyl molecular ion. The product ion spectra recorded when benzene molecular ion (*m*/*z* 78) collides at 30 eV with three different L−B films are shown in Figure 2. The spectra of DMSO-d_6 molecular ion (*m*/*z* 84) at 20 eV collisions with the same L−B films are given in Figure 3. As shown by these spectra, the $CF_3(CH_2)_n$-terminated L−B film gives results similar

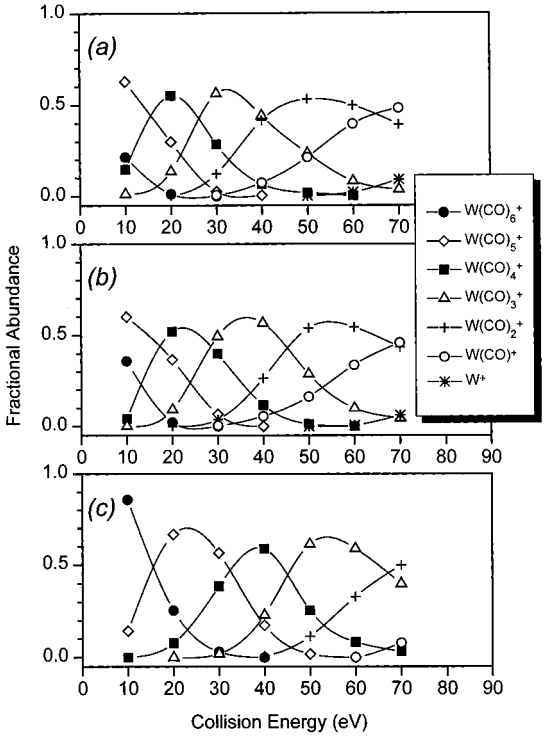

Figure 4. Energy-resolved mass spectra for surface-induced dissociation (SID) of $W(CO)_6^+$ with (a) *n*-$C_{13}F_{27}COOH$, (b) $CF_3(CH_2)_{16}COOH$, and (c) *n*-$C_{17}H_{35}COOH$ L−B films. The products of "chemical side reactions" other than the unimolecular dissociation of $W(CO)_6^+$ are not included (e.g., ion−surface reactions and chemical sputtering of surface species during SID). The total abundance of those "byproduct" ions increases in the raw spectra as collision energy increases (e.g., approximately 10% of the total scattered ions at 60 eV collisions with perfluorinated and $CF_3(CH_2)_n$-terminated L−B films, a little more than 20% at 70 collisions with the same two films).

to those for the perfluorinated film, but quite different from those for the stearate film. This is evident by the following three observations: (i) overall shape (product ion distribution) of the spectra, (ii) ratios of low mass fragments, and (iii) ion−surface reaction products.

It is seen in Figures 2 and 3 that the $CF_3(CH_2)_n$-terminated L−B film provides a percent fragmentation of the projectile ions similar to that given by the perfluorinated L−B film (Figures 2a vs 2b and 3a vs 3b), but different from that produced by collision with the stearate L−B film (Figures 2c and 3c). Furthermore, some low mass fragments that require relatively higher energies, such as $C_2H_2^+$ (*m*/*z* 26) from benzene (Figure 2a,b) and CD_3^+ (*m*/*z* 18) from DMSO-d_6 (Figure 3a,b), are present in SID spectra for both perfluorinated and $CF_3(CH_2)_n$-terminated L−B films, but are absent in the spectra for the stearate L−B film (Figures 2c and 3c). All of these results indicate that similar internal energy is deposited into the projectile ions with $CF_3(CH_2)_n$-terminated and perfluorinated L−B films.

The fragmentation patterns produced when the $W(CO)_6^+$ projectile ion collides with the films were used to estimate the percentage of kinetic energy transferred to internal energy (T → V). $W(CO)_6^+$ is an established "thermometer" ion (with a known unimolecular dissociation pattern and established dissociation energetics) that has been used for this purpose previously.[6,18,34,35,48,50] The energy-resolved SID mass spectra of $W(CO)_6^+$ (up to 70 eV) obtained with the three L−B film targets are illustrated in Figure 4. The trend observed with $W(CO)_6^+$ (Figure 4) for these three L−B films is the same as

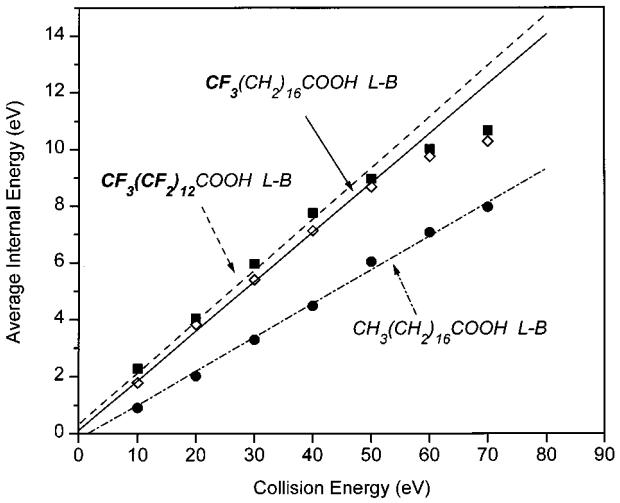

Figure 5. Estimated average internal energy deposited into $W(CO)_6^+$ during SID with three different L−B films as a function of collision energies. Two data points at 60 and 70 eV collisions with perfluorinated and $CF_3(CH_2)_n$-terminated L−B films are not included in the linear fit (see discussion in text).

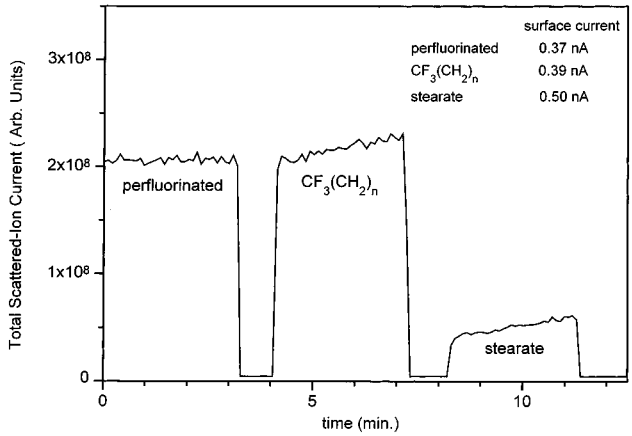

Figure 6. Total scattered-ion current (TIC) recorded by the detector of the SID tandem mass spectrometer when benzene molecular ions collide at 30 eV kinetic energy with three different L−B films.

that observed with the two small organic molecular ions (Figure 2 and 3). For example, the maximum abundance of the fragment $W(CO)_4^+$, formed by the loss of two CO molecules, occurs at approximately 20 eV collision energy with both perfluorinated and $CF_3(CH_2)_n$-terminated L−B films (Figure 4a,b), but at approximately 40 eV collision energy with the stearate film (Figure 4c). Using an algorithm previously published by Cooks and co-workers,[50,51] the distribution of internal energy deposited into $W(CO)_6^+$ at each collision energy was estimated. The weighted average of each estimated internal energy distribution is plotted against collision energy in Figure 5.

The estimated ratio of T → V for $W(CO)_6^+$ is determined as 18.1% (±1.5), 17.4% (±0.8), and 11.9% (±0.6) for the perfluorinated, $CF_3(CH_2)_n$-terminated, and stearate L−B films, respectively, assuming a linear fit is applicable (Figure 5). The errors listed in parentheses above represent twice the standard deviation of the least-squares linear fit shown in Figure 5, but do not represent the genuine error that could be caused by the algorithm for the estimation of the internal energies. The estimated T → V ratios for perfluorinated and $CF_3(CH_2)_n$-terminated L−B films are in good agreement with the previously reported value of 19−20% for the fluoroalkanethiolate SAM surface on gold prepared from $CF_3(CF_2)_{11}(CH_2)_2SH$,[18] and the reported value of 18% for liquid perfluoropolyether (PFPE) thin films on a metal.[34] Those cited values were obtained at a collision angle similar to that in our SID instrument and using the same algorithm as that employed for L−B films in this study. The estimated value for the stearate L−B film is comparable to the value of 11−13% for SID on stainless steel covered with adventitious hydrocarbons.[18,48] Different methods for the internal energy estimation other than the algorithm used in this study have also been published.[23,36,52] However, this study concerns mainly the trend in internal energy deposition among three L−B films and other estimation methods will not be discussed here.

Another point that must be made clear is that we do not intend to allege that the deposited internal energy as a function of the collision energy should be linear over a large range of energy, although a good linear relationship is shown in Figure 5 within a range of collision energies. However, we also *cannot* conclude that the ratio of T→ V decreases at the collision energies above 60 eV with perfluorinated and $CF_3(CH_2)_n$-terminated L−B films, just based on the deviation of two data points at 60 and 70 eV for those films. There are limitations of using a "thermometer" ion for the estimation of T→ V during SID: (i) "Chemical side reactions", such as ion−surface reactions and chemical sputtering during SID, occur and are not included in the estimation of internal energy. Significant errors could be caused if such "chemical side reactions" are not negligible. (ii)The maximum internal energy that can be estimated using a "thermometer" ion is limited by the molecular structures, dissociation pathways, and activation energies for dissociation. For example, the energy range that can be estimated with $W(CO)_6^+$ is about 13.0 eV (i.e., $W(CO)_6^+ \rightarrow W^+$, $E_0 = 13.0$ eV). As a consequence, when a "thermometer" ion with a small maximum limit range such as $Cr(CO)_6^+$ is used ($Cr(CO)_6^+ \rightarrow Cr^+$, $E_0 = 5.9$ eV), the observed deviation from linearity starts at even lower collision energies with perfluorinated and $CF_3(CH_2)_n$-terminated L−B films where no ion−surface reactions and chemical sputtering were observed (data not shown here).

Electron Transfer from Surface to Polyatomic Projectile Ions. Neutralization of projectile ions occurs by electron transfer from target surfaces during ion−surface collisions.[6,53] The relative tendency of three L−B films to cause neutralization of benzene molecular ions incident onto the films at 30 eV is presented in Figure 6. The figure is a plot of total scattered-ion currents (TIC) recorded when the precursor ions collide with the L−B films, measured with the electron multiplier detector of the SID tandem mass spectrometer**.** The total scattered-ions include intact precursor ions, ionic fragments, and ion−surface reaction product ions, in short, all the ions appearing in the spectra shown in Figure 2. The baseline in Figure 6 was recorded when the two filaments in the EI source (Extrel, Pittsburgh, PA) were turned off. Higher total scattered-ion currents (TIC) were recorded for perfluorinated and $CF_3(CH_2)_n$-terminated L−B films compared with that for the stearate film (Figure 6). This indicates less neutralization on both the perfluorinated film and the $CF_3(CH_2)_n$-terminated films than that on the stearate L−B film. The measurements reflected by the TIC curve are

(48) Wysocki, V. H.; Ding, J. M.; Jones, J. L.; Callahan, J. H.; King, F. L. *J. Am. Soc. Mass Spectrom.* **1992**, *3*, 27−32.
(49) Kane, T. E.; Angelico, V. J.; Wysocki, V. H. *Anal. Chem.* **1994**, *66*, 3733−3736, 4564−4564.
(50) Wysocki, V. H.; Kenttamaa, H. I.; Cooks, R. G. *Int. J. Mass Spectrom. Ion Process.* **1987**, *75*, 181−208.
(51) Dekrey, M. J.; Kenttamaa, H. I.; Wysocki, V. H.; Cooks, R. G. *Org. Mass Spectrom.* **1986**, *21*, 193−195.
(52) Vekey, K. *J. Mass Spectrom.* **1996**, *31*, 445−463.
(53) Cooks, R. G.; Ast, T.; Pradeep, T.; Wysocki, V. *Acc. Chem. Res.* **1994**, *27*, 316−323.

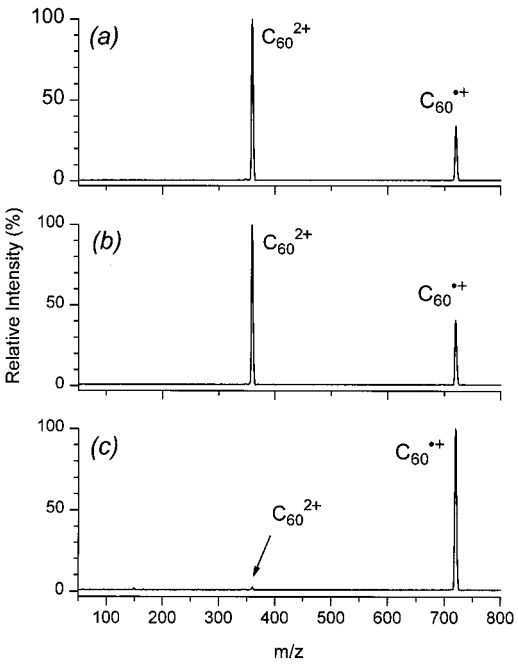

Figure 7. Spectra resulting from 80 eV collisions of C_{60}^{2+} (*m*/*z* 360) with L−B films prepared from (a) *n*-$C_{13}F_{27}COOH$, (b) $CF_3(CH_2)_{16}$-COOH, and (c) *n*-$C_{17}H_{35}COOH$.

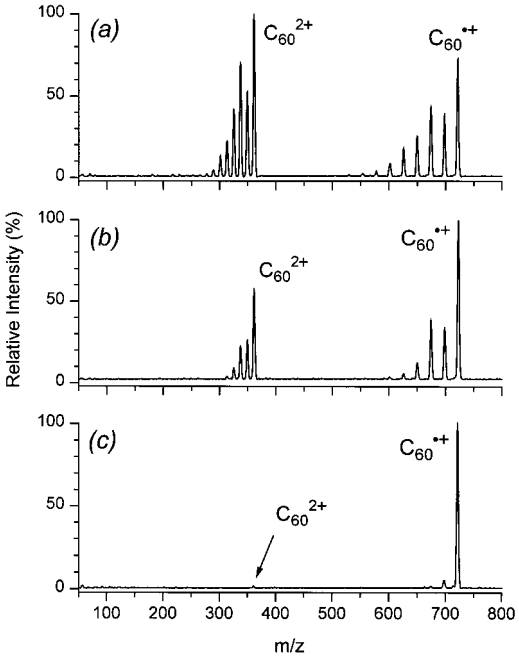

Figure 8. Spectra resulting from 220 eV collisions of C_{60}^{2+} (*m*/*z* 360) with the same films as those for Figure 7, i.e., (a) *n*-$C_{13}F_{27}COOH$, (b) $CF_3(CH_2)_{16}COOH$, and (c) *n*-$C_{17}H_{35}COOH$ L−B films.

in agreement with the current measured at the surface by a digital picoamperemeter connected to the target surface during the collisions. The higher the electric current at the target surface, the lower the ion current at the detector of the tandem mass spectrometer. For example, one set of measurement averages of surface current is recorded as 0.37 nA:0.39 nA: 0.50 nA for perfluorinated:$CF_3(CH_2)_n$-terminated:stearate L−B films, respectively. In summary, the efficiency of electron transfer from the films to benzene molecular ion follows the order perfluorinated ≈ $CF_3(CH_2)_n$-terminated < stearate L−B films.

The relative electron transfer from three L−B films was also investigated in a different way by using the C_{60} (buckminsterfullerene, "bucky ball") doubly charged molecular ion (C_{60}^{2+}, *m*/*z* 360). C_{60} was chosen because of its remarkable stability in the gas phase. One noteworthy example in the literature is that, in keV collisions with helium as target gas (keV CID), $C_{60}^{\bullet+}$ can encage a helium atom instead of fragmenting.[54,55] Due to the stability of C_{60}, almost no fragments are observed when 80 eV kinetic energy is applied in the collision of C_{60}^{2+} with the L−B films (Figure 7). The electron-transfer reaction measured is

$$C_{60}^{2+} + e\ [\text{from surface}] \rightarrow C_{60}^{\bullet+},\ RE\ (\approx -IE[C_{60}^{\bullet+}])$$

where RE is the recombination energy and IE the ionization energy. Many researchers have measured the IE of C_{60} by using various methods. For example, Scheier et al.[56] compiled 8 reported values for the first ionization energy of C_{60} (i.e., IE-[C_{60}], measured by six different methods) and 11 reported values for the second ionization energy of C_{60} (i.e., IE[$C_{60}^{\bullet+}$], measured by five different methods). Almost all measured IE[C_{60}] are consistent at 7.6 eV, whereas eleven reported IE[$C_{60}^{\bullet+}$] values range from approximately 9 to 12 eV with the arithmetic mean at ∼11.0 eV.[56] Regardless of the exact value, the second ionization energy of C_{60} is higher than, or at least comparable to, the expected ionization energy of the $CH_3(CH_2)_n$-terminated surface (e.g., IE[$C_{10}H_{22}$] = 9.7 eV). Thus, electron transfer from an alkyl-terminated surface to C_{60}^{2+} is expected to be exothermic. This is in agreement with the fact that more than 99% of the scattered ions recorded are $C_{60}^{\bullet+}$ ions when C_{60}^{2+} collides with the stearate L−B film (Figure 7c). In contrast, the expected higher ionization energy for the fluorocarbon surface (e.g., IE-[C_3F_8] = 13.4 eV) reduces the likelihood that electron transfer will occur when C_{60}^{2+} is incident on a fluorocarbon surface. As a result of the higher IE of the fluorocarbons, a large portion of the C_{60}^{2+} ions scatter from the surface without charge reduction (Figure 7a). Finally, more evidence for control of the electron transfer by the outermost group on the surfaces is that the $CF_3(CH_2)_n$-terminated L−B film gives a ratio of $C_{60}^{\bullet+}$:C_{60}^{2+} that is quite similar to that for the perfluorinated surface (Figure 7b vs 7a).

220 eV Collisions of C_{60}^{2+} with L−B Films. SID spectra of C_{60}^{2+} at 220 eV are given in Figure 8. At this SID collision energy, a number of fragment ion peaks at 12 or 24 u apart are present in the spectrum with the perfluorinated L−B film (Figure 8a). These peaks correspond to doubly or singly charged fragments that are produced either by loss of a single entity C_{2n}[57] or by the sequential loss of nC_2[58] from C_{60} ions. In contrast, the major fragment formed when C_{60}^{2+} collides with the stearate L−B film is seen as one peak of $[C_{60}-C_2]^+$ at a very low abundance (Figure 8c). The differences between the spectra acquired with the perfluorinated vs the stearate L−B films are similar to that reported previously using SAM surfaces of fluoroalkanethiolate vs alkanethiolate.[13] Even at this relatively higher collision energy, the $CF_3(CH_2)_n$-terminated L−B film

(54) (a) Weiske, T.; Bohme, D. K.; Hrusak, J.; Kratschmer, W.; Schwarz, H. *Angew. Chem., Int. Ed. Engl.* **1991**, *30*, 884−886. (b) Weiske, T.; Bohme, D. K.; Schwarz, H. *J. Phys. Chem.* **1991**, *95*, 8451−8452. (c) Weiske, T.; Hrusak, J.; Bohme, D. K.; Schwarz, H. *Chem. Phys. Lett.* **1991**, *186*, 459−462.

(55) Ross, M. M.; Callahan, J. H. *J. Phys. Chem.* **1991**, *95*, 5720−5723.

(56) Scheier, P.; Dunser, B.; Worgotter, R.; Lezius, M.; Robl, R.; Mark, T. D. *Int. J. Mass Spectrom. Ion Process.* **1994**, *138*, 77−93.

(57) McHale, K. J.; Polce, M. J.; Wesdemiotis, C. *J. Mass Spectrom.* **1995**, *30*, 33−38.

(58) Scheier, P.; Dunser, B.; Worgotter, R.; Muigg, D.; Matt, S.; Echt, O.; Foltin, M.; Mark, T. D. *Phys. Rev. Lett.* **1996**, *77*, 2654−2657.

still gives a SID spectrum more like that with the perfluorinated film (Figure 8b vs 8a), other than that with the stearate L−B film (Figure 8c), in terms of fragmentation of C_{60} and charge reduction from C_{60}^{2+} to $C_{60}^{\bullet+}$. Nonetheless, at this higher collision energy, a little more charge reduction and a little less fragmentation is provided by the $CF_3(CH_2)_n$-terminated film in comparison with the perfluorinated L−B film (Figure 8b vs 8a). The results of a molecular dynamics (MD) simulation done by Mowrey et al. show that the carbon lattice on a hydrogen-terminated diamond surface {111} is crumpled three layers deep during the impact of a neutral C_{60} at 200 or 250 eV.[59,60] In other words, the differences as shown with $CF_3(CH_2)_n$-terminated vs perfluorinated L−B films (Figure 8b vs 8a) indicate some significant contributions from the underlying $(CH_2)_n$ vs $(CF_2)_n$ for C_{60} collisions with L−B films at 220 eV.

Ion−Surface Reactions with L−B Films. DMSO-d_6 molecular ion (*m*/*z* 84) was chosen as a probe for hydrogen abstraction from the films (e.g., Figure 3c). Benzene molecular ion (*m*/*z* 78) is a good probe to investigate fluorine addition versus the addition of a hydrocarbon unit from the films, e.g., the product ions $C_6H_4F^+$ and $C_6H_5F^+$ (*m*/*z* 95 and 96, respectively; Figure 2a) versus the product ion $C_7H_7^+$ (*m*/*z* 91; Figure 2c). For the perfluorinated L−B film, a small amount of *m*/*z* 91 (not labeled, Figure 2a) and a small amount of [DMSO-d_6 + H]$^+$ (not labeled, Figure 3a) indicate that the film is slightly contaminated by hydrocarbon, either during the preparation or in the vacuum chamber (10^{-7} to 10^{-6} Torr pressure). The ratio of *m*/*z* 91 to *m*/*z* 95 and 96 in benzene spectra with the perfluorinated L−B film (Figure 2a) is similar to that with a fluoroalkanethiolate SAM on gold prepared by 12 h immersion of gold substrate in the fluoroalkanethiol solution (unpublished data in the Wysocki research group), whereas the same SAM surface prepared by 72 h immersion gives almost no *m*/*z* 91.[21] Note that hydrocarbon is much more reactive for the CH_x transfer to the projectile ions than fluorocarbon for the F addition. Therefore, the relative abundance of *m*/*z* 91 vs *m*/*z* 95 and& 96 (Figure 2a) does not represent the relative composition of two different species on the surface. With the $CF_3(CH_2)_n$-terminated L−B film, the reaction products are similar to (although not exactly the same as) those formed with the perfluorinated L−B films (Figures 2b vs 2a and 3b vs 3a). This suggests that the terminal group is also the main determinant of these atomic/group transfers to the polyatomic projectile ions, in addition to being the determinant of the energy transfer and electron transfer for polyatomic projectile ions as discussed in previous sections. A slightly higher CH_x/H adduct ion intensity for the $CF_3(CH_2)_n$-terminated L−B film relative to that for the perfluorinated film (Figures 2b vs 2a and 3b vs 3a) could be the result of several possible factors: First, the packing quality of the L−B film for 18,18,18-trifluorooctadecanoic acid and perfluoroteradecanoic acid could be slightly different and thus the films could have different amounts of defect sites, and/or, different tendencies for contamination after formation (e.g., in the vacuum chamber). Second, exposed methylenes of $CF_3(CH_2)_n-$ at surface defect sites or some disruption sites caused by ion impact could contribute to a slightly higher CH_x/H adduct ion intensity. Future investigation of these ion−surface reactions with the SAM surface of $CF_3(CH_2)_nSH$[43] on gold will be of interest. It is worth noting that a L−B film made from 12,12,-12-trifluorododecanoic acid [$CF_3(CH_2)_{10}COOH$] that does not form a "solid phase" on the air−water interface in the L−B trough (refer to Figure 1) gives a much higher intensity of *m*/*z* 91 vs *m*/*z* 95 and 96 for the product ion spectrum of benzene molecular ion (spectra not shown here). The percentage fragmentation is accordingly lower with the $CF_3(CH_2)_{10}COOH$ L−B film (spectra not shown here) than that obtained with the $CF_3(CH_2)_{16}COOH$ L−B film.

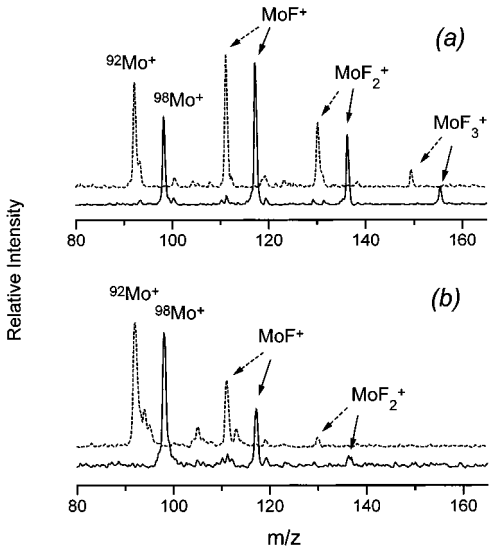

Figure 9. The metal atomic ion and its fluorine adduct ion region of the product ion spectra of Mo^+ incident at 60 eV kinetic energy on (a) *n*-$C_{13}F_{27}COOH$ and (b) $CF_3(CH_2)_{16}COOH$ L−B films. Solid line: isotope $^{98}Mo^+$ selected as the precursor ion. Dashed line: isotope $^{92}Mo^+$ selected as the precursor ion.

Fluorine addition to an atomic ion with the L−B films was investigated by using Mo^+ or Cr^+ ions as the projectile probes. Figure 9 shows the precursor ion and adduct ion regions of the product ion spectra for a $^{98}Mo^+$ (solid line) or $^{92}Mo^+$ (dashed line) incident at 60 eV onto the perfluorinated L−B film (part a) and $CF_3(CH_2)_n$-terminated L−B film (part b). Additions of multiple fluorine atoms to a Mo^+ projectile are seen with the perfluorinated L−B film (Figure 9a). The spectra obtained with perfluorinated L−B films are consistent with that previously reported by Cooks and co-workers using a fluoroalkanethiolate SAM surface of $CF_3(CF_2)_{11}(CH_2)_2SH$ on gold.[28] Cooks and co-workers suggested that some of the fluorine atoms in the additions come from the underlying $-CF_2-$ on the fluoroalkanethiol SAM surface (moreover, two or more of the multiple fluorine atoms could be from the same surface fluoroalkyl chain).[28] Arguments in their proposed mechanism include the following: (i) Some of the required energy for the endothermic processes of $M^+ \rightarrow MF_n^+$ could be provided by the energy released in the concomitant C═C bond formation on the surface (e.g., a double bond formed between two carbon atoms of terminal CF_3CF_2 by abstraction of one fluorine atom from each carbon) and (ii) the number of fluorine atoms in the additions and the relative intensities of the adduct ion peaks are dependent on the incident angle of the primary ion beam, with the maximum at the angle of the surface normal.[28] In other words, the multiple number of fluorine additions could be dependent on the penetration of the atomic metal ion into a depth of the surface to reach at least the first CF_2 unit underneath the terminal CF_3 group. According to their proposed mechanism,[28] the probability of fluorine additions would be predicted to decrease for the $CF_3(CH_2)_n$-terminated film. This is in agreement with the experimental observation that the adduct ion peaks are of lower intensities with $CF_3(CH_2)_n$-terminated vs perfluorinated L−B films (Figure 9b vs 9a). Similar results were also observed

(59) Mowrey, R. C.; Brener, D. W.; Dunlap, B. I.; Mintmire, J. W.; White, C. T. *J. Phys. Chem.* **1991**, *95*, 7138−7142.

(60) Beck, R. D.; John, P.; Alvarez, M. M.; Diederich, F.; Whetten, R. L. *J. Phys. Chem.* **1991**, *95*, 8402−8409.

with a $^{52}Cr^+$ ion (spectra not shown here). For example, the intensity ratio of Cr^+:CrF^+:CrF_2^+ is detected as 100:95:8.5 at 40 eV collision with the perfluorinated L−B, whereas no trace of CrF_2^+ is detected for 40 eV collision with the $CF_3(CH_2)_n$-terminated film and the ratio of Cr^+:CrF^+ is 100:19. The penetration of the atomic projectile ion into a depth of the $CF_3(CH_2)_n$-terminated film is confirmed by our observation of the extent of neutralization of Mo^+ and Cr^+ incident on the film. By comparison of total scattered-ion currents (TIC) measured for Mo^+ incident at 60 eV on the L−B films (TIC not shown here), the neutralization for 60 eV Mo^+ collisions with the films has the following order: perfluorinated L−B < $CF_3(CH_2)_n$-terminated L−B ≈ stearate L−B. This is also illustrated by different signal-to-noise ratios in Figure 9. Relative to that for the perfluorinated film, the signal-to-noise for the $CF_3(CH_2)_n$-terminated L−B is worse (Figure 9b vs 9a) due to the weaker signals (i.e., as a result of higher neutralization), although the resolution of the quadrupole mass analyzer was actually opened a little in the acquisition of the spectra for the $CF_3(CH_2)_n$-terminated L−B film. Based on the results discussed above, our experiments provide further evidence that could support the mechanisms proposed by Cooks and co-workers.[28] The similarity between $CF_3(CH_2)_n$- and $CH_3(CH_2)_n$-terminated films for electron transfer to the atomic ion Mo^+ at 60 eV collisions is in contrast to what is observed for polyatomic ions such as benzene molecular ion (Figure 6) and C_{60}^{2+} (Figure 7), and is consistent with penetration of *atomic* metal ions into the hydrocarbon portion of the $CF_3(CH_2)_n$− film. The observations discussed above suggest that there is a projectile-size dependence for the low-energy ion−surface interactions. The results of Ar^+ scattering from a SAM surface of $CF_3(CH_2)_{15}S$−Au, recently reported by Rabalais and co-workers,[44] also suggest the penetration of atomic Ar^+ ion into a few atomic layers of the surface.

Conclusions

The use of model surfaces, e.g., labeled by fluorine (this study) or by isotopes (our previous Communication to this journal) at the outermost carbon, is an effective way to investigate low-energy ion−surface interactions. Recent developments in preparation of new thiolate SAMs and new L−B films will lead to future research in this direction that will better characterize the ion−surface collision processes. In turn, the knowledge that is being and will be gained in the investigations of the ion−surface interactions with various model surfaces might lead to a surface characterization technique based on the interactions, e.g., to probe the outermost exposed surface groups or atomic layers.

Our results from this study support the previous speculation by many researchers that the effective mass of the surface controls the conversion of translational energy into internal modes of a polyatomic impinging ion. Moreover, our results suggest that the outermost surface group (e.g., CF_3 vs CH_3) is the main determinant of this energy transfer with fluorinated vs hydrocarbon-terminated surfaces for a low-energy (e.g., 10−100 eV) polyatomic projectile ion. On the other hand, it is still not clear whether the high electronegativity and low polarizability of fluorine plays a role in energy transfer. This question could be addressed in the future using a series of model surfaces terminated by fluorine vs chlorine vs bromine. At this point, our ability to understand the roles of underlying methylene/fluoromethylene chains or an assembly of the surface backbone chains in the conversion of translational energy into internal modes of a polyatomic ion is still limited. First, the physical processes of polyatomic ion−surface collisions can be very complicated. For example, multibody collision or collective collisions of a polyatomic ion with a number of atoms or groups on the surface can occur during the ion−surface impact. The orientation or average orientation of a polyatomic projectile ion during the impact can influence the energy transfer. Moreover, the time frames of the collisions (e.g., a low-energy polyatomic ion collision with organic thin films) are not yet well understood. Our experimental observations reported in this paper may encourage further experimental and theoretical investigations to better understand the processes.

The results of electron transfer (neutralization of a projectile ion) and atom/group transfer (ion−surface reaction) to an impinging ion are distinctive for polyatomic ions vs atomic ions. For polyatomic ions, the outermost surface group seems to be the main determinant for the efficiency of these transfers. The trends for different L−B films toward the electron transfer to a polyatomic ion, investigated in the absence of solvent and electric double-layer effects, might provide information relevant to studies of electron transfer at electrode−solution interfaces and increase our knowledge of electron transfer through organic thin films. Our results for neutralization and ion−surface reaction of an *atomic* ion, together with ion scattering and ion−surface reaction results reported by other researchers, suggest the penetration of an atomic impinging ion into a depth of the films (e.g., the methylene portion of a $CF_3(CH_2)_n$-terminated film).

Acknowledgment. Financial support of this work from the National Science Foundation (CHE-9224719) is acknowledged. The use of the L−B trough in the laboratory of Dr. S. Scott Saavedra at the University of Arizona and discussions with him regarding the preparation of L−B films are gratefully appreciated. Vincent J. Angelico is acknowledged for the assistance with reproducing TIC measurements of benzene SID.

JA990719A